Available online at www.sciencedirect.com
SCIENCE DIRECT
Journal of Catalysis 239 (2006) 501–506
JOURNAL OF CATALYSIS
www.elsevier.com/locate/jcat

Research Note

Toward computational screening in heterogeneous catalysis: Pareto-optimal methanation catalysts

Martin P. Andersson [a], Thomas Bligaard [a], Arkady Kustov [b], Kasper E. Larsen [c], Jeffrey Greeley [a], Tue Johannessen [c], Claus H. Christensen [b], Jens K. Nørskov [a,*]

[a] *Center for Atomic-Scale Materials Physics, Department of Physics, NanoDTU, Technical University of Denmark, DK-2800 Lyngby, Denmark*
[b] *Center for Sustainable and Green Chemistry, Department of Chemistry, NanoDTU, Technical University of Denmark, DK-2800 Lyngby, Denmark*
[c] *Department of Chemical Engineering, NanoDTU, Technical University of Denmark, DK-2800 Lyngby, Denmark*

Received 20 January 2006; revised 13 February 2006; accepted 18 February 2006

Available online 24 March 2006

Abstract

Finding the solids that are the best catalysts for a given reaction is a daunting task due to the large number of combinations and structures of multicomponent surfaces. In addition, it is not only the reaction rate that needs to be optimized; the selectivity, durability, and cost must also be taken into account. Here we propose a computational screening approach and apply it to design a new metal alloy catalyst for the methanation reaction ($CO + 3H_2 \rightarrow CH_4 + H_2O$).

Keywords: Alloy; Bimetallic; Methanation; Hydrogenation; Fischer–Tropsch; DFT; Design; Screening; Optimization; Pareto

1. Introduction

It has been shown that the kinetics of full catalytic reactions can be described semiquantitatively on the basis of thermochemistry and activation energies calculated using density functional theory (DFT) [1–3]. If such an approach could be extended from a single catalyst to a range of catalysts, then DFT calculations could be used for a first screening of new catalysts. Although this is not yet possible, we take a step in that direction with the following procedure. First, we establish a correlation between the catalytic activity and a *descriptor*, which we can calculate directly using DFT. The descriptor is chosen on the basis of a general understanding of parameters determining the variation in catalytic activity from one catalyst to the next [4,5]. We use experimental data for the activity of a set of elemental metals to determine the optimum value of the descriptor. Next, we perform a preliminary screening of a number of intermetallic alloys based on a model of the effect of alloying developed from DFT calculations. Then we study the most interesting alloys using full DFT calculations to verify the alloy model and make definite predictions of the activity. Finally, we synthesize the best catalyst candidates and measure their catalytic activity.

To illustrate this approach, we use the methanation reaction ($CO + 3H_2 \rightarrow CH_4 + H_2O$). This is one of the classic reactions in heterogeneous catalysis [6–9] used in connection with, for instance, catalytic ammonia synthesis ($N_2 + 3H_2 \rightarrow 2NH_3$) to remove trace amounts of CO from the hydrogen feed gas. It has attracted renewed interest for the clean up of reformate hydrogen fuels for low-temperature fuel cells in which CO is a strong poison [10]. The traditional methanation catalyst is Ni supported on Al_2O_3 [9]. The reaction is well described experimentally [11,12] and theoretically [5, 13,14], and recently experimental high-throughput screening methods have been applied to find new catalysts for this reaction [15].

* Corresponding author. Fax: +45 45 93 23 99.
E-mail address: norskov@fysik.dtu.dk (J.K. Nørskov).

0021-9517/$ – see front matter
doi:10.1016/j.jcat.2006.02.016

2. Methods

2.1. Computational details

2.1.1. Electronic structure calculations

The electronic structure calculations are carried out using DFT calculations [16,17] in a plane wave pseudopotential implementation [18,19]. Ultra-soft pseudopotentials [20] are used to represent the ionic cores, allowing for a reasonable treatment of first-row atoms and transition metals even with a relatively limited plane wave basis. The plane wave cutoff in the calculations is 25 Rydberg for the wave functions and 50 Rydberg for the electron densities, except for Co, for which the plane wave cutoff is 35 Rydberg and the density cutoff 70 Rydberg. For Fe, Co, and Ni, the calculations are spin-polarized. The calculations are performed using the RPBE exchange correlation [21] on periodically repeated stepped fcc(211) metal slabs with 12 layers in the [211] direction. This corresponds to 4 close-packed layers and gives 24 atoms in the unit cell. This particular choice of model allows us to retain the correct bulk composition and periodic structure for the ordered binary 1:3 and 1:1 alloys (such as $FeNi_3$ and FeNi), as well as for the regular fcc structures. In all cases, the uppermost close-packed layer (3 [211]-layers) is fully relaxed together with the adsorbed species. The lattice constants are chosen as the calculated bulk lattice constant for the respective metals in their ground state structure using the RPBE functional. There is at least 10 Å of vacuum between the slabs, and the dipole interaction between the periodically repeated slabs is decoupled by introducing a dipole layer in the vacuum between the slabs. A k-point sampling of $4 \times 4 \times 1$ Monkhorst–Pack k-points [22] is chosen.

The calculations are performed with one adsorbate per unit cell, that is, a surface coverage of 1/6 monolayers, or equivalently a step coverage of 0.5. All transition states (TS) are found using a constrained bond optimization technique, which for both Ni(211) and Ru(211) is found to give the same energy as the more rigorous nudged elastic band method [23].

2.1.2. Oxygen–surface alloy binding energies

The raw data for the oxygen binding energy (BE_O) on binary surface alloys, along with the computational details, have been provided previously [24]. The alloys are constructed by allowing incorporation of various coverages of solute atoms into the surface layers of assorted hosts. From this database of DFT-based BE_O, two interpolative schemes to estimate BE_O values are developed. For the first scheme, the interpolated BE_O is simply taken as the average of the BE_O on the pure metals surrounding the threefold sites. For example, the BE_O on a PtPtPd threefold site (in which the substrate of the surface alloy can be either Pt or Pd) would be estimated as $(2BE_O(\text{pure Pt}) + BE_O(\text{pure Pd}))/3$. The particular alloys analyzed with this interpolative scheme (taken from a larger database in Ref. [24]) are selected by requiring that the oxygen atom move by no more than 0.05 unit cell vectors ($\sim 1/15$ of a lattice constant) from the threefold sites during relaxation, that the lattice constants of the pure metals composing each alloy differ by no more than 0.2 Å, and that the surface alloys contain only mixed (not pure) solute overlayers. Thus, a total of 62 surface alloys are considered. For the second scheme, the interpolated binding energies are again calculated as an average of the BE_O's. In this case, however, the basic data used for the interpolation come from pure overlayers, not pure metals. For example, the BE_O of a PtPtPd-on-Pt alloy (in which Pt is the substrate) would be $(2BE_O(\text{PtPtPt-on-Pt} + BE_O(\text{PdPdPd-on-Pt}))/3$. This scheme thus rigorously accounts for strain and electronic structure effects of the substrate element on the surface elements. The surface alloys analyzed in this scheme include all of the alloys analyzed in the first scheme plus additional alloys resulting from the elimination of the lattice constant restriction (102 in total).

2.2. Experimental details

2.2.1. Catalyst preparation

Spinel, $MgAl_2O_4$, a support with particle sizes of 0.25–0.40 mm, a pore volume of about 0.7 cm^3/g, and a surface area of 70 m^2/g, is used as a carrier material. Supported Ni/Fe catalysts are prepared using incipient wetness impregnation of the chosen sieve fraction of the support with aqueous solutions of the corresponding nitrates. Before impregnation, the support is dried in an oven at 200 °C for 5 h. A period of about 4 h is allowed for the salt solution to completely fill the pores of the carrier. The impregnated spinel is then dried at room temperature for 12 h and heated in air to 450 °C at a rate of 2.5 °C/min and kept at 450 °C for 3 h.

2.2.2. CO hydrogenation

The catalytic performance of the prepared catalysts is tested in CO hydrogenation. In a representative catalytic test, 150 mg of the catalyst (fraction 0.25–0.40 mm) is placed into the quartz plug-flow U-tube reactor between two layers of quartz wool. The flow of 2 vol% CO in H_2 is then admitted to the reactor at an hourly space velocity of about 40,000 h^{-1} and a reaction pressure of 1.0–1.1 bar. Before the activity measurements, the catalysts are reduced at 500 °C for 4 h, after which the temperature is lowered while the concentrations of CO, methane and other products are monitored using a Shimadzu gas chromatograph equipped with thermal conductivity and flame ionization detectors. The results of the activity measurements are calculated as mol CO converted per mol of metal in the catalyst per second,

$$\text{rate} = \frac{X_{CO} \cdot F_{CO}}{n_{cat}},$$

where X_{CO} is the fractional conversion of CO, F_{CO} denotes the molar feed rate of CO (mol/s), and n_{cat} is the total molar amount of metal in the catalyst used in the activity test.

3. Results

3.1. Computational results

Following the analysis reported previously [5], the two important properties of a metal surface in determining the rate of the methanation process are the barrier for CO dissociation and

the stability of the main intermediates on the surface, atomic C and O. Extensive DFT calculations of these parameters for different metal surfaces have shown them to be linearly correlated in what is called the Brønsted–Evans–Polanyi (BEP) relation [5], as shown in Fig. 1a. The reason for the correlation is that the C–O bond in the transition state for dissociation is so extended that it is very final state-like, thus leaving the transition state with bonding properties that vary like those of adsorbed atomic C and O. This means that one independent descriptor of the reactivity can be chosen as the dissociation energy of adsorbed CO, E_{diss}: the energy of C + O on the surface relative to the energy of adsorbed CO [25].

A BEP relation typically leads to a volcano-shaped dependence of the rate on E_{diss} [5]; see Fig. 1. For weak adsorption (the right leg of the volcano), the barrier for dissociation is high and limits the rate, whereas strong adsorption must lead to low rates of removal of adsorbed C and O from the surface to form the reaction products. This is illustrated in Fig. 1b, which shows experimentally measured rates on a number of supported elemental metal catalysts [5] as a function of the calculated E_{diss} on the most active step sites of the metals. The optimum value of E_{diss} can be seen to be $E_{\mathrm{diss}}(\mathrm{optimal}) = 0.06$ eV.

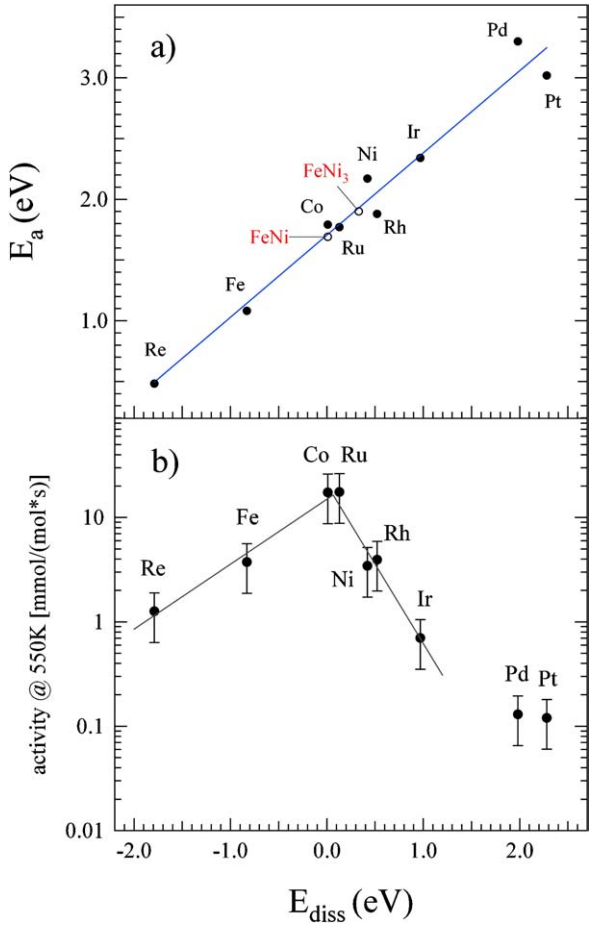

Fig. 1. (a) Brønsted–Evans–Polanyi (BEP) relation for the activation energy for CO dissociation vs the (adsorbed) CO dissociation energy, E_{diss}, at steps on the close packed surface of the metals. Pure metals are shown in full circles, and the two ordered alloys, FeNi and $FeNi_3$, are shown in hollow circles. The blue solid line (web version) is a best linear fit for the pure metals. (b) Measured catalytic activities for supported metal catalysts (adapted from Ref. [5]) are shown vs. E_{diss}. All energies are related to the molecularly adsorbed CO state at the step.

Having established that E_{diss} is a good descriptor for the catalytic activity and having found its optimum value, we now screen a number of catalysts, M, for their value of $\Delta E_{\mathrm{diss}}(\mathrm{M}) = |E_{\mathrm{diss}}(\mathrm{M}) - E_{\mathrm{diss}}(\mathrm{optimal})|$. We base our screening on a database of values of E_{diss} for the elemental metals calculated using DFT [4]. We calculate the values for an alloy surface using an interpolation model in which the adsorption energy, E_{ads}, at a site with a fraction x of A neighbors and a fraction $(1-x)$ of B neighbors is calculated as $E_{\mathrm{ads}}(\mathrm{A}_x\mathrm{B}_{1-x}) = xE_{\mathrm{ads}}(\mathrm{A}) + (1-x)E_{\mathrm{ads}}(\mathrm{B})$ [24,26,27]. We tested the model for the adsorption energy of atomic oxygen on the threefold sites of close-packed surfaces of a variety of surface alloys; Fig. 2 shows the results. The model gives rise to errors in the 0.1–0.2 eV range compared with full DFT calculations. Comparing this error with the range of energies, E_{diss}, in Fig. 1 shows that this is a useful accuracy for a first screening. When studying the most promising candidates in more detail later in this paper, we show that the interpolation concept works well for these systems.

We consider bulk alloys of the composition $\mathrm{A}_x\mathrm{B}_{1-x}$ ($x = 0$, 0.25, 0.5, 1), where A and B can be any of the metals Ni, Pd, Pt, Co, Rh, Ir, Fe, Ru, or Re. This creates a total of 117 different catalysts in our study. We make the further approximation that the bulk concentration, x, also indicates the range of concentration of element metal A in the surface site. We have verified that this is a good approximation for the two most interesting alloys in the study.

The interpolation model immediately suggests candidates for good alloy catalysts by combining elements on the left leg and the right leg of the volcano in Fig. 1. Here we use a more systematic approach in which we can include other important factors in the problem. As mentioned in Section 1, catalyst optimization is usually a multiobjective optimization problem in which it is not a priori possible to weigh the importance of different factors in a single measure. We illustrate this by considering not only the catalytic activity, but also the price of the catalyst. Multiobjective optimization problems are common in the economics literature, where a common solution is to use the Pareto-optimal set, as defined by the economist V. Pareto [28,29]. The Pareto-optimal set is the set of solutions that are nondominated in the sense that it is impossible to choose another solution and improve one property without making another property worse.

Fig. 3 shows a plot of the methanation activity measure, ΔE_{diss}, and price for all 117 catalyst materials in our study. Each alloy is represented by a point, and the Pareto-optimal set is indicated. The figure shows that very good catalysts, such as Ru, can be created, but these are also very expensive. If, on the other hand, cost is the main concern, then a less active catalyst, like Fe, is the best candidate. Ni lies somewhere in between Ru and Fe and thus represents a compromise if only pure metals are considered. Clearly, the Ni–Fe alloys stand out because they form a “knee” in the Pareto set, making the neighboring solutions in the Pareto

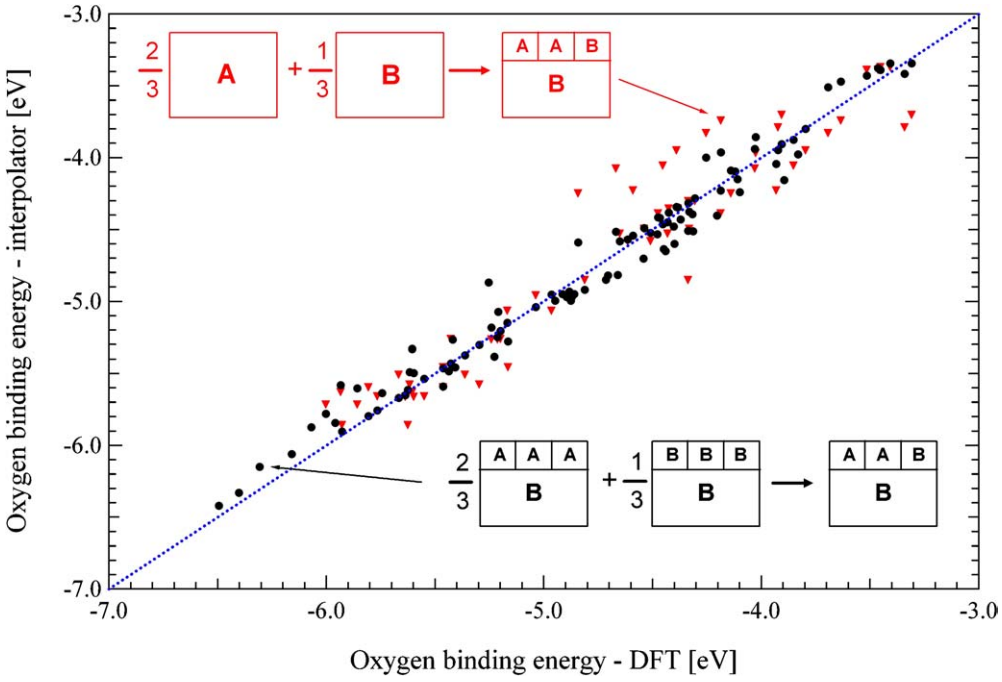

Fig. 2. All data points correspond to threefold site oxygen adsorption on heterogeneous binary surface alloys constructed from the same elemental metals as in Fig. 1 (pure metal overlayers are not included). Red triangles: interpolated values are estimated from arithmetic averaging of the appropriate pure metal binding energies. Alloys with components having lattice constants differing by less than 0.2 Å are shown. The average error is 0.17 eV. This scheme does not rigorously account for, e.g., strain differences between the pure metals and the surface alloys. Filled circles: interpolated values are estimated from arithmetic averaging of binding energies on pure overlayers on the appropriate metal substrate. This scheme thus accounts rigorously for strain and electronic structure effects, and the average error is 0.1 eV. Bulk alloys are expected to be in between these two limits, since they always have lattice constants intermediate between the corresponding constants of the pure metals composing the alloy.

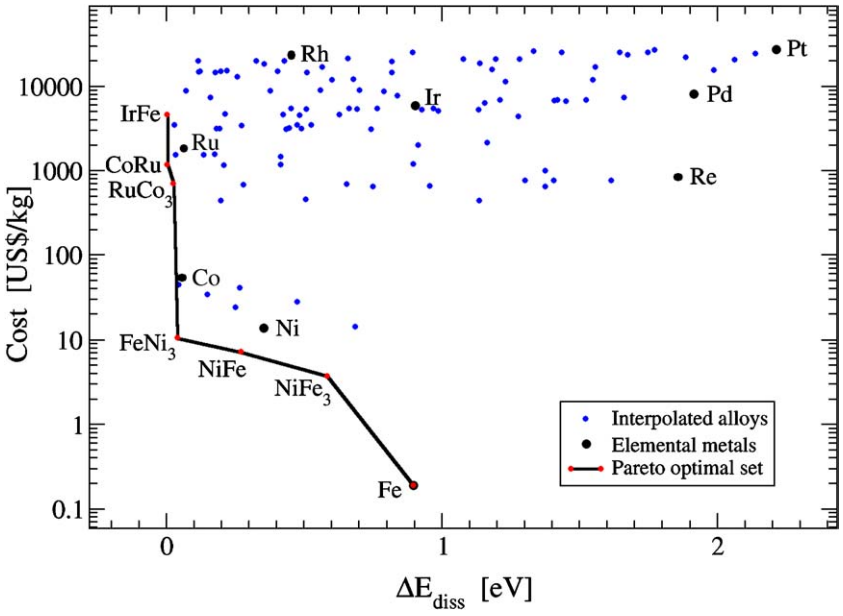

Fig. 3. Pareto plot of the activity measure $\Delta E_{\mathrm{diss}}(\mathrm{M}) = |E_{\mathrm{diss}}(\mathrm{M}) - E_{\mathrm{diss}}(\mathrm{optimal})|$ and the cost for 117 elemental metals and bimetallic alloys of the form $\mathrm{A}_x\mathrm{B}_{1-x}$ ($x = 0$, 0.25, 0.50, 1). Each blue point corresponds to a particular alloy. The elemental metals are shown (black), and the Pareto optimal set is also indicated (red). The cost of the bimetallic alloys has been approximated by the current commodity price of the constituent elemental metals [37].

set considerably worse in one respect or the other. Consequently, we studied the Ni_3Fe and NiFe alloys in more detail.

Fig. 1a includes the activation energy and dissociation energy for CO on step sites on Ni_3Fe and NiFe. It can be seen that the interpolation method works quite well; the value for the alloys is between Ni and Fe and even follows the bulk concentration x; the point for Ni_3Fe is closest to the main component, Ni, whereas the point for NiFe is close to the midpoint between Fe and Ni. Therefore, the full DFT calculation supports the

model behind Fig. 2 and clearly predicts that both Ni_3Fe and NiFe should be good candidates for catalysts with an activity higher than the constituents and close to that of the best catalysts, Ru and Co. For Ni_3Fe, our thermodynamic analysis of the free energies of the surface under reaction conditions found that the structure included in Fig. 1 is the most stable.

3.2. Experimental results

The Ni–Fe catalysts are synthesized and tested as described in the Methods section, and the reaction rates are plotted as a function of the Fe content in Fig. 4. The experiments completely confirm the predictions from computational screening. Depending slightly on temperature and concentration, the maximum activity is found either for Ni_3Fe or in between Ni_3Fe and NiFe. The measured value of the catalytic activity for the new Ni_3Fe-based catalyst is almost as good as that for Co, and it is considerably cheaper. Considering that no attempt has been made to optimize the preparation method and activation procedure, this finding must be considered quite promising.

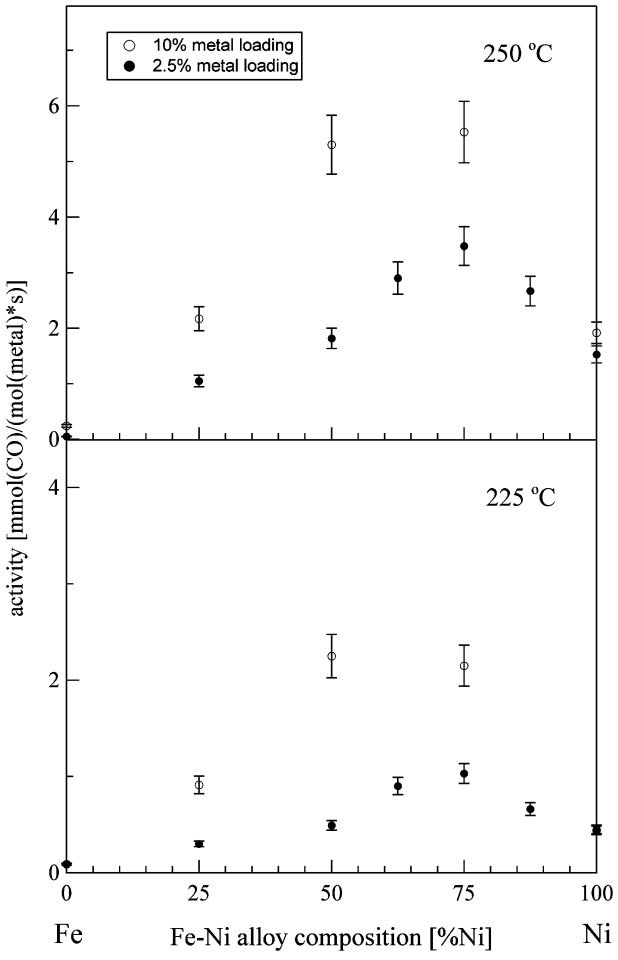

Fig. 4. Measured rate of CO removal for a gas containing 2% CO in 1 bar of H_2 as a function of the Fe content in FeNi alloy catalysts. Results are shown for two different temperatures and two metal concentrations.

4. Discussion

Fe–Ni alloys have been found to have good catalytic properties for a partial oxidation of methane to syngas [30], and the catalytic activity of Fe–Ni alloys has also been tested for other hydrogenation reactions of carbon-containing compounds, such as CO_2 methanation [31] and benzene hydrogenation [32], with varying success. In particular, it has been found that Ni–Fe alloys are good for CO hydrogenation under Fischer–Tropsch conditions (i.e., high CO pressure) [33]. Based on this finding, it may not be very surprising that Fe–Ni alloys are superior methanation catalysts. Still, we note that even a recent state-of-the-art experimental high-throughput screening search for methanation catalysts did not find the results shown in Fig. 4 [15].

Under the conditions of the present experiments corresponding to the situation in which small amounts of CO (or CO_2) are removed from an H_2 stream, the best catalysts all have methane as the prime product (>90% selectivity). In view of the renewed interest in Fischer–Tropsch synthesis in connection with the production of clean diesel and other fuels [10,34], it would be interesting to extend the present analysis to include high CO pressures, at which the product distribution is quite different. This cannot be done trivially, however, because the optimum value of E_{diss} determining the overall rate is expected to depend on the reaction conditions [35] and because for Fischer–Tropsch synthesis, the selectivity is often more interesting than the overall turnover.

The predictive power of the DFT calculations relies strongly on the fact that the width of the volcano-like relation in Fig. 1b is of the order several tenths of an eV—a general finding making rates of complete catalytic reactions considerably less sensitive to systematic errors in calculated interaction energies than the rate of each of the individual reaction steps [2,3,36]. This is an accuracy that can be routinely obtained by current versions of the exchange-correlation functional [21].

5. Conclusion

In conclusion, we have shown that it is possible to establish quantitative descriptors for the catalytic activity of the methanation reaction by combining catalytic measurements with DFT calculations of appropriate properties of the catalyst surface. We can then use DFT calculations and models developed based on these calculations to screen for new catalysts with better catalytic performance. Synthesis and testing of these catalysts revealed that they are superior to the conventional Ni catalyst. We have also shown that it is possible to perform multivariable optimization of catalyst properties, and suggest that the concept of the Pareto-optimal set may be useful in catalyst development.

A number of challenges remain in the development of an entirely computational approach to catalyst optimization. The first of these challenges is to provide a completely ab initio determination of the optimum value for the descriptor. This will entail the development of a reliable kinetic model. The second challenge is to calculate the descriptor parameter directly using DFT rather than using the interpolation model applied

here. Finally, it is clear that the reaction that we have studied is extremely simple, and then more complex reactions with a multitude of products will be considerably more demanding. For such complex systems, we suggest that for the foreseeable future, optimal use of the available computer power will probably dictate using a hierarchy of computational approaches, such as those illustrated here.

Acknowledgments

The authors acknowledge support from the Danish Research Agency (grant 26-04-0047) and the Danish Center for Scientific Computing (grant HDW-1103-06). M.P. Andersson acknowledges a Marie Curie Fellowship through EU grant MEIF-CT-2004-011121. J. Greeley acknowledges a H.C. Ørsted Postdoctoral Fellowship from the Technical University of Denmark. The Center for Sustainable and Green Chemistry is sponsored by the Danish National Research Foundation.

References

[1] S. Linic, M.A. Barteau, J. Am. Chem. Soc. 125 (2003) 4034.
[2] K. Reuter, D. Frenkel, M. Scheffler, Phys. Rev. Lett. 93 (2004) 116105.
[3] K. Honkala, A. Hellman, I.N. Remediakis, A. Logadottir, A. Carlsson, S. Dahl, C.H. Christensen, J.K. Nørskov, Science 307 (2005) 555.
[4] J.K. Nørskov, T. Bligaard, A. Logadottir, S. Bahn, L.B. Hansen, M. Bollinger, H. Bengaard, B. Hammer, Z. Sljivancanin, M. Mavrikakis, Y. Xu, S. Dahl, C.J.H. Jacobsen, J. Catal. 209 (2002) 275.
[5] T. Bligaard, J.K. Nørskov, S. Dahl, J. Matthiesen, C.H. Chistensen, J. Sehested, J. Catal. 224 (2004) 206.
[6] P. Sabatier, J.B. Senderens, C. R. Acad. Sci. Paris 134 (1902) 514.
[7] M.A. Vannice, J. Catal. 50 (1977) 228.
[8] G.A. Somorjai, Introduction to Surface Chemistry and Catalysis, Wiley, New York, 1994.
[9] J. Sehested, S. Dahl, J. Jacobsen, J.R. Rostrup-Nielsen, J. Phys. Chem. B 109 (2005) 2432.
[10] S. Takenaka, T. Shimizu, K. Otsuka, Int. J. Hydrogen Energy 29 (2004) 1065.
[11] D.W. Goodman, R.D. Kelley, T.E. Madey, J.T. Yates Jr., J. Catal. 63 (1980) 226.
[12] T. Zubkov, G.A. Morgan Jr., J.T. Yates Jr., O. Kuhlert, M. Lisowski, R. Schillinger, D. Fick, H.J. Jansch, Surf. Sci. 526 (2003) 57.
[13] R.A. van Santen, A. de Koster, T. Koerts, Catal. Lett. 7 (1990) 1.
[14] M. Mavrikakis, M. Bäumer, H.J. Freund, J.K. Nørskov, Catal. Lett. 81 (2002) 153.
[15] K. Yaccato, R. Carhart, A. Hagemeyer, A. Lesik, P. Strasser, A.F. Volpe, H. Turner, H. Weinberg, R.K. Grasselli, C. Brooks, App. Catal. A: Gen. 296 (2005) 30.
[16] P. Hohenberg, W. Kohn, Phys. Rev. 136 (1964) B864.
[17] W. Kohn, L.J. Sham, Phys. Rev. 140 (1965) A1133.
[18] M.C. Payne, M.P. Teter, D.C. Allan, T.A. Arias, J.D. Joannopoulos, Rev. Mod. Phys. 64 (1992) 1045.
[19] J.G. Kresse, J. Furtmüller, Comput. Mater. Sci. 6 (1996) 15.
[20] D. Vanderbilt, Phys. Rev. B 41 (1990) 7892.
[21] B. Hammer, L.B. Hansen, J.K. Nørskov, Phys. Rev. B 59 (1999) 7413.
[22] H.J. Monkhorst, J.D. Pack, Phys. Rev. B 13 (1976) 5188.
[23] G. Mills, H. Jonsson, G.J. Schenter, Surf. Sci. 324 (1995) 305.
[24] J. Greeley, J.K. Nørskov, Surf. Sci. 592 (2005) 104.
[25] In the present paper we employ a different descriptor, E_{diss}, than in Ref. [5]. Now E_{diss} is evaluated with respect to the strongly adsorbed CO precursor state instead of CO in the gas-phase.
[26] C.J.H. Jacobsen, S. Dahl, B.S. Clausen, S. Bahn, A. Logadottir, J.K. Nørskov, J. Am. Chem. Soc. 123 (2001) 8404.
[27] P. Liu, J.K. Nørskov, Phys. Chem. Chem. Phys. 3 (2001) 3814.
[28] V. Pareto, Manuale di Economia Politica, Societa Editrice Libraria, Milano, 1906, translated to English as: V. Pareto, Manual of Political Economy, Macmillan, New York, 1971.
[29] T. Bligaard, G.H. Johannesson, A.V. Ruban, H.L. Skriver, K.W. Jacobsen, J.K. Nørskov, Appl. Phys. Lett. 83 (2003) 4527.
[30] J.G. Wang, C.J. Liu, Y.P. Zhang, K.L. Yu, X.L. Zhu, F. He, Catal. Today 89 (2004) 183.
[31] S. Mori, W.C. Xu, T. Ishidzuki, N. Ogasawara, J. Imai, K. Kobayashi, Appl. Catal. A: Gen. 137 (1996) 255.
[32] B.H. Zeifert, J. Salmones, J.A. Hernandez, R. Reynoso, N. Nava, J.G. Cabanas-Moreno, G. Aguilar-Rios, Catal. Lett. 63 (1999) 161.
[33] T. Ishihara, K. Eguchi, H. Arai, Appl. Catal. 30 (1987) 225.
[34] M.E. Dry, Appl. Catal. A: Gen. 276 (2004) 1.
[35] C.J.H. Jacobsen, S. Dahl, A. Boisen, B.S. Clausen, H. Topsoe, A. Logadottir, J.K. Nørskov, J. Catal. 205 (2002) 382.
[36] T. Bligaard, K. Honkala, A. Logadottir, J.K. Nørskov, S. Dahl, C.J.H. Jacobsen, J. Phys. Chem. B 107 (2003) 9325.
[37] Average 2004 metal prices taken from the U.S. Geological Survey: Mineral Commodity Summaries, http://minerals.usgs.gov/minerals/pubs/mcs/.